Dynamical calculation of the ΔΔ dibaryon candidates

Hongxia Huang,[1] Jialun Ping,[1,*] and Fan Wang[2]
[1]*Department of Physics, Nanjing Normal University, Nanjing 210097, People's Republic of China*
[2]*Department of Physics, Nanjing University, Nanjing 210093, People's Republic of China*
(Received 21 January 2014; published 3 March 2014)

We perform a dynamical calculation of the ΔΔ dibaryon candidates with $IJ^P = 03^+$ and $IJ^P = 30^+$ in the framework of two constituent quark models: the quark delocalization color screening model and the chiral quark model. Our results show that the dibaryon resonances with $IJ^P = 03^+$ and $IJ^P = 30^+$ can be formed in both models. The mass and width of $IJ^P = 03^+$ state are smaller than that of $IJ^P = 30^+$ state due to the one-gluon-exchange interaction between quarks. The resonance mass and decay width of $IJ^P = 03^+$ state in both models agree with that of the recently observed resonance in the reaction $pn \to d\pi^0\pi^0$. The $IJ^P = 30^+$ ΔΔ is another dibaryon candidate with smaller binding energy and larger width. The hidden-color channel coupling is added to the chiral quark model, and we find it can lower the mass of the dibaryons by 10−20 MeV.

DOI: 10.1103/PhysRevC.89.034001 PACS number(s): 13.75.Cs, 12.39.Pn, 12.39.Jh, 14.20.−c

I. INTRODUCTION

The possibility of dibaryon states was first proposed by Dyson and Xuong [1] in 1964. However, this topic got considerable attention only after Jaffe's prediction of the H particle in 1977 [2]. All quark models, including lattice QCD calculations, predict that in addition to $q\bar{q}$ mesons and q^3 baryons, there should be multiquark systems $(q\bar{q})^2$, $q^4\bar{q}$, q^6, quark-gluon hybrids $q\bar{q}g$, q^3g, and glueballs [3]. A worldwide theoretical and experimental effort to search for dibaryon states with and without strangeness has lasted a long time. The $S = 0$, $J^P = 0^-$ d' dibaryon, which is hard to explain by quark models [4], was claimed by experiments in 1993 and disappeared years later [5]. Our group showed that the $S = 0$, $I = 0$, $J = 3$ d^* is a tightly bound six-quark system rather than a loosely bound nucleuslike system of two Δs [6–9]. The recent Faddeev equation calculation supports the existence of d^* [10]. An $S = -3$, $I = 1/2$, $J = 2$ $N\Omega$ state was proposed as a high strangeness dibaryon candidate [11]. Kopeliovich predicted high strangeness dibaryons, such as the di-Ω with $S = -6$, using the flavor SU(3) Skyrmion model [12]. Zhang *et al.* suggested searching for the di-Ω in ultrarelativistic heavy-ion collisions [13]. La France and Lomon predicted a deuteronlike dibaryon resonance using R-matrix theory [14] and measurements at Saclay seem to offer experimental support for its existence [15]. Despite numerous claims, there has not been a well-established experimental candidate for these dibaryon states.

However, the interest in the H particle have been revived recently by lattice QCD calculations of different collaborations, NPLQCD [16] and HALQCD [17]. These two groups reported that the H particle is indeed a bound state at pion mass larger than the physical one. Then, Carames and Valcarce examined the H particle within a chiral constituent quark model and obtained a bound H dibaryon with $B_H = 7$ MeV [18].

Recently, a pronounced resonance structure has been observed in pn collisions leading to two-pion production in the reaction $pn \to d\pi^0\pi^0$, which suggests the presence of an $IJ^P = 03^+$ subthreshold ΔΔ resonance, called henceforth d^*, with a resonance mass $M = 2.37$ GeV and a width $\Gamma \approx 70$ MeV [19,20]. The relatively large binding energy of this state shows that it is much closer to these interesting multiquark states than a loosely bound system such as the deuteron. However, the width is remarkably smaller than that given by a naive model estimate $\Gamma_\Delta \lesssim \Gamma \lesssim 2\Gamma_\Delta$, where $\Gamma_\Delta \approx 120$ MeV.

According to Ref. [1], in addition to d^*, one should also have a state with mirrored quantum numbers for spin and isospin, i.e., $IJ^P = 30^+$, called D_{30} in Ref. [1]. Recently, Bashkanov *et al.* further pointed out that the observation of the d^* resonance state raises the possibility of producing other novel six-quark dibaryon configurations allowed by QCD and showed the D_{30} state could be regarded as manifestations of hidden-color six-quark configurations in QCD [21]. To what extent does such kind of spin-isospin symmetry exist in hadron spectroscopy? It should be an interesting check of the Goldstone boson exchange model where the isospin triplet π exchange interaction has the spin-isospin symmetry [22]. On the other hand, many former quark model calculations showed that the mass of $IJ^P = 03^+$ ΔΔ state was much smaller than that of $IJ^P = 30^+$ ΔΔ state because these models include the effective gluon exchange. In the quark delocalization color screening model (QDCSM) the $IJ^P = 03^+$ state is bound by 320 MeV, while the $IJ^P = 30^+$ state is bound by only 48 MeV [9]. By using the standard confinement and one gluon exchange (OGE) interaction model, Maltman found the $IJ^P = 03^+$ state is bound by 260 MeV, while the $IJ^P = 30^+$ state is bound by only 30 MeV [23]. Both results are in qualitative agreement with the results of Oka and Yazaki [24,25], Cvetic [26], Valcarce [27] and Zhang [28]. This situation calls for a more quantitative study of the $IJ^P = 30^+$ state.

Quantum chromodynamics (QCD) is widely accepted as the fundamental theory of the strong interaction. However,

*Corresponding author: jlping@njnu.edu.cn

the direct use of QCD for low-energy hadronic interactions, for example, the nucleon-nucleon (NN) interaction, is still difficult because of the nonperturbative complications of QCD. QCD-inspired quark models are still the main approach to study the baryon-baryon interaction. The effective single gluon exchange interaction model can describe the properties of ground-state baryons, the repulsive core of NN interaction. For excited states of baryons, it does not work as well as for the ground states. The Goldstone boson exchange interaction is often included to improve the quark model. In the present work, we are interested in the ground-state dibaryons, and it is expected that the quark model can work well. The most commonly used quark model in the study of baryon-baryon interaction is the chiral quark model (ChQM) [27,29,30], in which the σ meson is indispensable to provide the intermediate-range attraction. Another quark-model approach is the QDCSM [7], which has been developed with the aim of understanding the well-known similarities between nuclear and molecular forces despite the obvious energy and length scale differences. In this model, the intermediate-range attraction is achieved by the quark delocalization, which is like the electron percolation in the molecules. The color screening is needed to make the quark delocalization possible and it might be an effective description of the hidden color channel coupling [31]. Therefore, to study the D_{30} state with QDCSM is especially interesting because its special relation to the hidden color channel effect. We have showed that both QDCSM and ChQM give a good description of the S and D wave phase shifts of NN ($IJ = 01$) scattering and the properties of deuteron [32] despite the difference of the mechanism of the NN intermediate-range attraction. Recently, the d^* resonances in NN D-wave scattering were restudied with the QDCSM and ChQM [33]. Both models give $IJ^P = 03^+$ $\Delta\Delta$ resonances reasonable well. Therefore, we use these two models to calculate the mass and decay width of the D_{30} dibaryon and compare the result with the d^* resonance to check if there is a D_{30} dibaryon state. The hidden color channels are added to the ChQM to check their effect in the $\Delta\Delta$ system.

The structure of this paper is as follows. A brief introduction of two quark models is given in Sec. II. Section III is devoted to the numerical results and discussions. The last section is a summary.

II. TWO QUARK MODELS

A. Chiral quark model

The Salamanca version of ChQM is chosen as the representative of the chiral quark models. It has been successfully applied to hadron spectroscopy and NN interaction. The model details can be found in Ref. [27]. Only the Hamiltonian and parameters are given here. The ChQM Hamiltonian in the nucleon-nucleon sector is

$$
\begin{aligned}
H &= \sum_{i=1}^{6}\left(m_i + \frac{p_i^2}{2m_i}\right) - T_c + \sum_{i<j}[V^G(r_{ij}) + V^\pi(r_{ij}) + V^\sigma(r_{ij}) + V^C(r_{ij})],\\
V^G(r_{ij}) &= \frac{1}{4}\alpha_s \boldsymbol{\lambda}_i\cdot\boldsymbol{\lambda}_j\left[\frac{1}{r_{ij}} - \frac{\pi}{m_q^2}\left(1+\frac{2}{3}\boldsymbol{\sigma}_i\cdot\boldsymbol{\sigma}_j\right)\delta(r_{ij}) - \frac{3}{4m_q^2 r_{ij}^3}S_{ij}\right] + V_{ij}^{G,LS},\\
V_{ij}^{G,LS} &= -\frac{\alpha_s}{4}\boldsymbol{\lambda}_i\cdot\boldsymbol{\lambda}_j\frac{1}{8m_q^2}\frac{3}{r_{ij}^3}[\mathbf{r}_{ij}\times(\mathbf{p}_i-\mathbf{p}_j)]\cdot(\boldsymbol{\sigma}_i+\boldsymbol{\sigma}_j),\\
V^\pi(r_{ij}) &= \frac{1}{3}\alpha_{ch}\frac{\Lambda^2}{\Lambda^2-m_\pi^2}m_\pi\left\{\left[Y(m_\pi r_{ij}) - \frac{\Lambda^3}{m_\pi^3}Y(\Lambda r_{ij})\right]\boldsymbol{\sigma}_i\cdot\boldsymbol{\sigma}_j + \left[H(m_\pi r_{ij}) - \frac{\Lambda^3}{m_\pi^3}H(\Lambda r_{ij})\right]S_{ij}\right\}\boldsymbol{\tau}_i\cdot\boldsymbol{\tau}_j,\\
V^\sigma(r_{ij}) &= -\alpha_{ch}\frac{4m_u^2}{m_\pi^2}\frac{\Lambda^2}{\Lambda^2-m_\sigma^2}m_\sigma\left[Y(m_\sigma r_{ij}) - \frac{\Lambda}{m_\sigma}Y(\Lambda r_{ij})\right] + V_{ij}^{\sigma,LS},\\
V_{ij}^{\sigma,LS} &= -\frac{\alpha_{ch}}{2m_\pi^2}\frac{\Lambda^2}{\Lambda^2-m_\sigma^2}m_\sigma^3\left[G(m_\sigma r_{ij}) - \frac{\Lambda^3}{m_\sigma^3}G(\Lambda r_{ij})\right][\mathbf{r}_{ij}\times(\mathbf{p}_i-\mathbf{p}_j)]\cdot(\boldsymbol{\sigma}_i+\boldsymbol{\sigma}_j),\\
V^C(r_{ij}) &= -a_c\boldsymbol{\lambda}_i\cdot\boldsymbol{\lambda}_j\left(r_{ij}^2+V_0\right) + V_{ij}^{C,LS},\\
V_{ij}^{C,LS} &= -a_c\boldsymbol{\lambda}_i\cdot\boldsymbol{\lambda}_j\frac{1}{8m_q^2}\frac{1}{r_{ij}}\frac{dV^c}{dr_{ij}}[\mathbf{r}_{ij}\times(\mathbf{p}_i-\mathbf{p}_j)]\cdot(\boldsymbol{\sigma}_i+\boldsymbol{\sigma}_j), \quad V^c = r_{ij}^2,\\
S_{ij} &= \frac{(\boldsymbol{\sigma}_i\cdot\mathbf{r}_{ij})(\boldsymbol{\sigma}_j\cdot\mathbf{r}_{ij})}{r_{ij}^2} - \frac{1}{3}\boldsymbol{\sigma}_i\cdot\boldsymbol{\sigma}_j,
\end{aligned}
\tag{1}
$$

where S_{ij} is quark tensor operator; $Y(x)$, $H(x)$, and $G(x)$ are standard Yukawa functions; and T_c is the kinetic energy of the center of mass. All other symbols have their usual meanings. The parameters of ChQM are given in Table I.

B. Quark delocalization color screening model

The model and its extension were discussed in detail in Refs. [7,8]. Its Hamiltonian has the same form as Eq. (1) but without σ meson exchange and a phenomenological color

TABLE I. Parameters of quark models.

	ChQM	QDCSM
$m_{u,d}$ (MeV)	313	313
b (fm)	0.518	0.518
a_c (MeV fm^{-2})	46.938	56.755
V_0 (fm^2)	−1.297	−0.5279
μ (fm^{-2})	–	0.45
α_s	0.485	0.485
m_π (MeV)	138	138
α_{ch}	0.027	0.027
m_σ (MeV)	675	–
Λ (fm^{-1})	4.2	4.2

screening confinement potential is used:

$$V^C(r_{ij}) = -a_c \boldsymbol{\lambda}_i \cdot \boldsymbol{\lambda}_j [f(r_{ij}) + V_0] + V_{ij}^{C,LS},$$
$$f(r_{ij}) = \begin{cases} r_{ij}^2 & \text{if } i,j \text{ occur in the same baryon orbit,} \\ \frac{1-e^{-\mu r_{ij}^2}}{\mu} & \text{if } i,j \text{ occur in different baryon orbits.} \end{cases} \quad (2)$$

Here, μ is the color screening constant to be determined by fitting the deuteron mass in this model. The quark delocalization in QDCSM is realized by replacing the left-(right-) centered single Gaussian functions, the single-particle orbital wave function in the usual quark cluster model,

$$\phi_\alpha(\vec{S}_i) = \left(\frac{1}{\pi b^2}\right)^{3/4} e^{-\frac{1}{2b^2}(\vec{r}_\alpha - \vec{S}_i/2)^2}, \quad (3)$$

$$\phi_\beta(-\vec{S}_i) = \left(\frac{1}{\pi b^2}\right)^{3/4} e^{-\frac{1}{2b^2}(\vec{r}_\beta + \vec{S}_i/2)^2}, \quad (4)$$

with delocalized ones,

$$\psi_\alpha(\vec{S}_i,\epsilon) = (\phi_\alpha(\vec{S}_i) + \epsilon\phi_\alpha(-\vec{S}_i))/N(\epsilon),$$
$$\psi_\beta(-\vec{S}_i,\epsilon) = (\phi_\beta(-\vec{S}_i) + \epsilon\phi_\beta(\vec{S}_i))/N(\epsilon), \quad (5)$$
$$N(\epsilon) = \sqrt{1+\epsilon^2+2\epsilon e^{-S_i^2/4b^2}}.$$

The mixing parameter $\epsilon(\vec{S}_i)$ is not an adjusted one but determined variationally by the dynamics of the multiquark system itself. This assumption allows the multiquark system to choose its most favorable configuration in a larger Hilbert space, so the ansatz for the wave functions [Eq. (5)] is a generalization of the usual quark cluster model ones, which enlarges the variational space for the variational calculation. It has been used to explain the cross-over transition between hadron phase and quark-gluon plasma phase [34]. The model parameters are fixed as follows: The u,d-quark mass difference is neglected and $m_u = m_d$ is assumed to be exactly 1/3 of the nucleon mass, namely $m_u = m_d = 313$ MeV. The π mass takes the experimental value. The Λ takes the same values as in Ref. [27], namely $\Lambda = 4.2$ fm^{-1}. The chiral coupling constant α_{ch} is determined from the πNN coupling constant through

$$\alpha_{ch} = \left(\frac{3}{5}\right)^2 \frac{g_{\pi NN}^2}{16\pi} \frac{m_\pi^2}{m_N^2}. \quad (6)$$

The other parameters b, a_c, V_0, and α_s are determined by fitting the nucleon and Δ masses and the stability of nucleon size $\frac{\partial M_N}{\partial b} = 0$. All parameters used are listed in Table I. In order to compare the intermediate-range attraction mechanism, the σ meson exchange in ChQM and quark delocalization and color screening in QDCSM, the same values of parameters b, α_s, α_{ch}, m_u, m_π, and Λ are used for these two models. Thus, these two models have exactly the same contributions from one-gluon-exchange and π exchange. The only difference of the two models comes from the short- and intermediate-range part, σ exchange for ChQM, and quark delocalization and color screening for QDCSM.

III. RESULTS AND DISCUSSIONS

The resonating group method (RGM), described in more detail in Ref. [35], is used to calculate the masses and decay widths of two-baryon states with $IJ^P = 03^+$ and $IJ^P = 30^+$. The channels involved are listed in Table II. Here the baryon symbol is used only to denote the isospin; the superscript denotes the spin, $2S+1$, and the subscript "8" denotes color-octet, so $^2\Delta_8$ means the $I,S = 3/2,1/2$ color-octet state.

Because an attractive potential is necessary for forming bound state or resonance, we first calculate the effective potentials of the S-wave $\Delta\Delta$ states. The effective potential between two colorless clusters is defined as

$$V(s) = E(s) - E(\infty), \quad (7)$$

where $E(s)$ is the diagonal matrix element of the Hamiltonian of the system in the generating coordinate. The effective potentials of the S-wave $\Delta\Delta$ for $IJ^P = 03^+$ and $IJ^P = 30^+$ cases within two quark models are shown in Figs. 1(a) and 1(b). From Fig. 1, we can see that the potentials are attractive for both $IJ^P = 03^+$ and $IJ^P = 30^+$ $\Delta\Delta$ states, and the attraction of the $IJ^P = 03^+$ state is larger than that of $IJ^P = 30^+$ state in two models. The difference of attraction between $IJ^P = 03^+$ and $IJ^P = 30^+$ in QDCSM is larger than that in ChQM.

In order to study what leads to the different effective potentials between $IJ^P = 03^+$ and $IJ^P = 30^+\Delta\Delta$ states,

TABLE II. The two-baryon channels for states with $IJ^P = 03^+$ and 30^+.

$IJ^P = 03^+$	1 $\Delta\Delta(^7S_3)$	2 $NN(^3D_3)$	3 $\Delta\Delta(^3D_3)$	4 $\Delta\Delta(^7D_3)$		
	5 $^2\Delta_8\ ^2\Delta_8(^3D_3)$	6 $^4N_8\ ^4N_8(^3D_3)$	7 $^4N_8\ ^2N_8(^3D_3)$	8 $^2N_8\ ^2N_8(^3D_3)$	9 $^4N_8\ ^4N_8(^7S_3)$	10 $^4N_8\ ^4N_8(^7D_3)$
$IJ^P = 30^+$	1 $\Delta\Delta(^1S_0)$	2 $\Delta\Delta(^5D_0)$	3 $^2\Delta_8\ ^2\Delta_8(^1S_0)$			

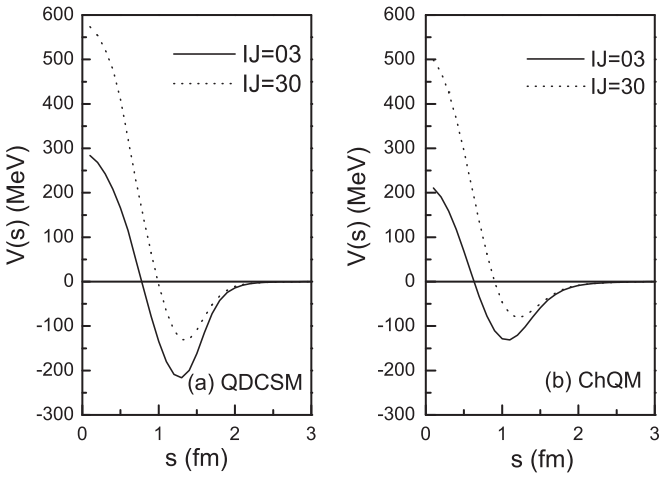

FIG. 1. The potentials of S-wave $\Delta\Delta$ for $IJ^P = 03^+$ and $IJ^P = 30^+$ cases within two quark models.

the contributions to the effective potential from the kinetic energy, confinement, one gluon exchange (OGE) and one boson exchange potentials are calculated. We find that all the contributions are the same between $IJ^P = 03^+$ and $IJ^P = 30^+$ $\Delta\Delta$ states, except for the contribution from OGE potential, which are shown in Fig. 2. From Figs. 2(a) and 2(b), we can see that OGE potential of $IJ^P = 03^+$ $\Delta\Delta$ state is attractive in both QDCSM and ChQM, while OGE potential of $IJ^P = 30^+\Delta\Delta$ state is repulsive in both QDCSM and ChQM. Obviously, the difference comes from the color-magnetic part of OGE interaction [$V^G(r_{ij})$ in Eq. (1)]. The color-magnetic part contains the color and spin operator: $-\boldsymbol{\lambda}_i \cdot \boldsymbol{\lambda}_j \boldsymbol{\sigma}_i \cdot \boldsymbol{\sigma}_j$. The matrix elements of the operator for the two states $IJ^P = 03^+$ and $IJ^P = 30^+$ can be evaluated as follows:

$$V_{03} = -(6\sigma_s c_s + 9\sigma_s c_a - 6\sigma_s c_s), \quad (8)$$

$$V_{30} = -(6\sigma_a c_s + 9\sigma_s c_a - 6\sigma_s c_s). \quad (9)$$

Here, $\sigma_s = 1$, $\sigma_a = -3$, $c_s = \frac{4}{3}$, $c_a = -\frac{8}{3}$. From Eqs. (5) and (6), we can see that the difference of the contributions from

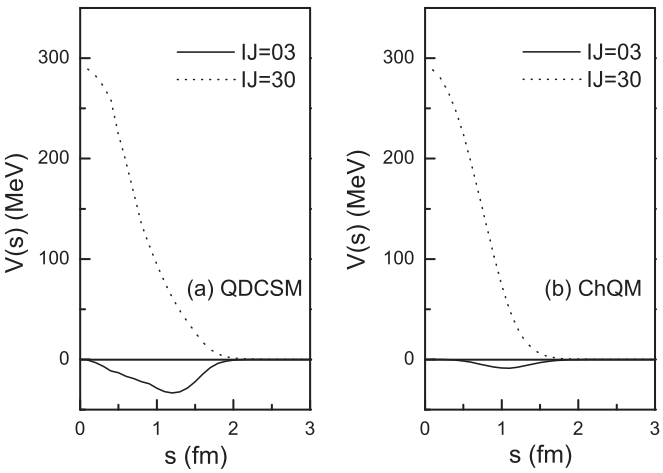

FIG. 2. The OGE potentials of S-wave $\Delta\Delta$ for $IJ^P = 03^+$ and $IJ^P = 30^+$ cases within two quark models.

TABLE III. $\Delta\Delta$ or resonance mass M and decay width Γ, in MeV, in two quark models for the $IJ^P = 03^+$ state.

	QDCSM		ChQM		
	sc	4 cc	sc	4 cc	10 cc
M	2365	2357	2425	2413	2393
Γ_{NN}	–	14	–	14	14
Γ_{inel}	103	96	177	161	136
Γ	103	110	177	175	150

OGE between $IJ^P = 03^+$ and $IJ^P = 30^+$ states comes from the first term of these two expressions: $-6\sigma_s c_s = -6 \times 1 \times \frac{4}{3} = -8$ in V_{03} and $-6\sigma_a c_s = -6 \times (-3) \times \frac{4}{3} = 24$ in V_{30}, which leads to the attractive OGE potential in $IJ^P = 03^+$ case and the repulsive OGE potential in $IJ^P = 30^+$ case. So if one does not include OGE interaction, the same result will be obtained in $IJ^P = 03^+$ and $IJ^P = 30^+$ S-wave $\Delta\Delta$ states.

In order to see whether or not there is any bound state, a dynamic calculation is needed. Here the RGM equation is employed. Expanding the relative motion wave function between two clusters in the RGM equation by Gaussians, the integrodifferential equation of RGM can be reduced to algebraic equation, the generalized eigenequation. The energy of the system can be obtained by solving the eigenequation. In the calculation, the baryon-baryon separation ($|\mathbf{s}_n|$) is taken to be less than 6 fm (to keep the matrix dimension manageably small).

For the $IJ^P = 03^+$ state, the binding energy of $\Delta\Delta$, resonance mass, and decay width listed in Table III are taken from our previous calculation [33]; sc stands for the single channel $\Delta\Delta(^7S_3)$ calculation; 4 cc and 10 cc stand for channel-coupling calculations, "4" denotes the four color-singlet channels listed in Table II, and "10" denotes the ten channels (four color-singlet channels and six hidden-color channels) listed in Table II. Γ_{NN} is the decay width of $\Delta\Delta(^7S_3) \to NN(^3D_3)$; Γ_{inel} is the inelastic width caused by decaying Δs [33] and Γ stands for the total decay width $\Gamma = \Gamma_{NN} + \Gamma_{\text{inel}}$. For the $IJ^P = 30^+$ state, since it cannot decay into NN or $NN\pi$ but only into the $NN\pi\pi$ channel, we only calculate the inelastic width Γ_{inel} here. The binding energy of $IJ^P = 30^+$ state and decay width $\Gamma = \Gamma_{\text{inel}}$ are listed in Table IV; sc stands for the single channel $\Delta\Delta(^1S_0)$ calculation; channel coupling calculations are denoted by 2 cc (two color-singlet channels) and 3 cc (two color-singlet channels and one hidden-color channel). There are several features which are discussed below.

TABLE IV. $\Delta\Delta$ mass M and decay width Γ, in MeV, in two quark models for the $IJ^P = 30^+$ state.

	QDCSM		ChQM		
	sc	2 cc	sc	2 cc	3 cc
M	2430	2423	2457	2450	2440
Γ	185	175	228	216	200

First, from Tables III and IV, we can see that both the individual $IJ^P = 03^+$ and $IJ^P = 30^+\Delta\Delta$ are bound in QDCSM and ChQM, which indicates that the attraction between two Δs is strong enough to bind two Δs together. However, the mass of $IJ^P = 03^+$ state is smaller than that of $IJ^P = 30^+$ state, due to the OGE interaction as mentioned above. This result is in qualitative agreement with the results of our previous study [9], Oka and Yazaki [24,25], Cvetic [26], Valcarce [27], and Zhang [28] as mentioned above. For the decay width, take the QDCSM results as an example, the inelastic width $\Gamma_{\rm inel}$ of $IJ^P = 03^+$ state is 79 MeV smaller than that of $IJ^P = 30^+$ state, because of the smaller mass of $IJ^P = 03^+$ state. Although the $IJ^P = 03^+$ state can decay to $NN(^3D_3)$ state, the decay width is only 14 MeV, so the total decay width of the $IJ^P = 03^+$ ΔΔ is 110 MeV, which is still 65 MeV smaller than that of the $IJ^P = 30^+$ state. The mass and width of the $IJ^P = 03^+$ state are both smaller than that of the $IJ^P = 30^+$ state. The resonance mass and decay width of the $IJ^P = 03^+$ state indicate that this resonance is a promising candidate for the observed isoscalar ABC structure recently reported by the CELSIUS-WASA Collaboration [19] and WASA-at-COSY Collaboration [20]. The $IJ^P = 30^+$ state is another possible six-quark dibaryon state and it might be observed in proper experiments as discussed in Ref. [21].

Second, the similar results are obtained in ChQM. However, both $IJ^P = 03^+$ and $IJ^P = 30^+$ states have smaller mass and decay width in QDCSM than in ChQM. Our hidden color channel coupling calculation in the *NN* scattering shows that the color screening assumed in QDCSM is an effective description of the hidden-color channel coupling effects [31]. To check the effect of hidden-color channels coupling in ChQM, the hidden-color channels are added to ChQM. For the $IJ^P = 03^+$ state, the six hidden-color channels coupling lowers the ChQM resonance mass by 20 MeV. For the $IJ^P = 30^+$ state, the one hidden-color channel coupling lowers the ChQM mass by 10 MeV. After including the hidden-color channel coupling the resonance masses in ChQM are closer to that in QDCSM. So in the ΔΔ system the hidden-color channel coupling effect is also to increase the attraction, which is consistent with our previous conclusion that the hidden-color channel coupling might be responsible for the intermediate-range attraction of *NN* interaction [31].

IV. SUMMARY

In the present work, we perform a dynamical calculation of the ΔΔ dibaryon candidates with $IJ^P = 03^+$ and $IJ^P = 30^+$ in the framework of QDCSM and ChQM. Our results show that the attractions between two Δs is strong enough to bind two Δs together for both $IJ^P = 03^+$ and $IJ^P = 30^+$. However, the mass and width of the $IJ^P = 03^+$ state are smaller than those of the $IJ^P = 30^+$ state due to the OGE interaction. The resonance mass and decay width of the $IJ^P = 03^+$ state indicate that this ΔΔ resonance is a promising candidate for the recently observed one in the ABC effect. The $IJ^P = 30^+$ ΔΔ is another possible six-quark dibaryon state and it might be observed in proper experiments, such as $pp \to D_{30}\pi^-\pi^- \to (pp\pi^+\pi^+)\pi^-\pi^-$, which can be done at COSY and JPARC [21].

The naive expectation of the spin-isospin symmetry is broken by the effective one gluon exchange between quarks. The d^* and D_{30} states searching will be another check of this gluon exchange mechanism and the Goldstone boson exchange model.

QDCSM and ChQM obtained similar results. However, the mass and decay width of $IJ^P = 03^+$ and $IJ^P = 30^+$ dibaryons in QDCSM are smaller than those in ChQM. By including the hidden-color channels in ChQM, the resonance masses are lowered by 10–20 MeV. This fact shows once more that the quark delocalization and color screening used in QDCSM might be an effective description of the hidden-color channel coupling.

ACKNOWLEDGMENT

This work is supported partly by the National Science Foundation of China under Contracts No. 11205091, No. 11035006, and No. 11175088.

[1] F. J. Dyson and N. H. Xuong, Phys. Rev. Lett. **13**, 815 (1964).
[2] R. L. Jaffe, Phys. Rev. Lett. **38**, 195 (1977).
[3] R. L. Jaffe, Phys. Rep. **409**, 1 (2005); F. E. Close, Int. J. Mod. Phys. A **20**, 5156 (2005).
[4] A. J. Buchmann, G. Wagner, and A. Faessler, Phys. Rev. C **57**, 3340 (1998); J. L. Ping, F. Wang, and T. Goldman, *ibid.* **62**, 054007 (2000), and references therein.
[5] R. Bilger, H. A. Clement, and M. G. Schepkin, Phys. Rev. Lett. **71**, 42 (1993); **72**, 2972 (1994); W. Brodowski *et al.*, Phys. Lett. B **550**, 147 (2002).
[6] T. Goldman, K. Maltman, G. J. Stephenson, K. E. Schmidt, and F. Wang, Phys. Rev. C **39**, 1889 (1989).
[7] F. Wang, G. H. Wu, L. J. Teng, and T. Goldman, Phys. Rev. Lett. **69**, 2901 (1992).
[8] F. Wang, J. L. Ping, G. H. Wu, L. J. Teng, and T. Goldman, Phys. Rev. C **51**, 3411 (1995); J. L. Ping, H. R. Pang, F. Wang, and T. Goldman, *ibid.* **65**, 044003 (2002); J. L. Ping, F. Wang, and T. Goldman, Nucl. Phys. A **657**, 95 (1999); **688**, 871 (2001).
[9] H. R. Pang, J. L. Ping, F. Wang, and T. Goldman, Phys. Rev. C **65**, 014003 (2001).
[10] A. Gal and H. Garcilazo, Phys. Rev. Lett. **111**, 172301 (2013).
[11] T. Goldman, K. Maltman, G. J. Stephenson, K. E. Schmidt, and F. Wang, Phys. Rev. Lett. **59**, 627 (1987).
[12] V. B. Kopeliovich, Nucl. Phys. A **639**, 75c (1998).
[13] Z. Y. Zhang, Y. W. Yu, C. R. Ching, T. H. Ho, and Z. D. Lu, Phys. Rev. C **61**, 065204 (2000).
[14] P. LaFrance and E. L. Lomon, Phys. Rev. D **34**, 1341 (1986), and references therein.
[15] F. Lehar, in *Baryons 98*, edited by D. W. Menze and B. Ch. Metsch (World Scientific, Singapore, 1999), p. 622.
[16] S. R. Beane, E. Chang, W. Detmold *et al.*, Phys. Rev. Lett. **106**, 162001 (2011).
[17] T. Inoue, N. Ishii, S. Aoki *et al.*, Phys. Rev. Lett. **106**, 162002 (2011).
[18] T. F. Carames and A. Valcarce, Phys. Rev. C **85**, 045202 (2012).

[19] M. Bashkanov *et al*. (CELSIUS-WASA Collaboration), Phys. Rev. Lett. **102**, 052301 (2009).
[20] P. Adlarson *et al*. (WASA-at-COSY Collaboration), Phys. Rev. Lett. **106**, 242302 (2011).
[21] M. Bashkanov, S. J. Brodsky, and H. Clement, Phys. Lett. B **727**, 438 (2013).
[22] L. Ya. Glozman and D. O. Riska, Phys. Rep. **268**, 263 (1996).
[23] K. Maltman, Nucl. Phys. A **438**, 669 (1985).
[24] M. Oka and K. Yazaki, Phys. Lett. B **90**, 41 (1980).
[25] M. Oka, in *Frontiers of High Energy Spin Physics*, edited by T. Hasegawa, N. Horikawa, A. Masaike, and S. Sawada (Universal Academy Press, Tokyo, 1993), p. 590.
[26] M. Cvetic *et al*., Phys. Lett. B **93**, 489 (1980).
[27] A. Valcarce, H. Garcilazo, F. Fernandez, and P. Gonzalez, Rep. Prog. Phys. **68**, 965 (2005), and references therein.
[28] Q. B. Li, P. N. Shen, Z. Y. Zhang, and Y. W. Yu, Nucl. Phys. A **683**, 487 (2001).
[29] Y. Fujiwara, C. Nakamoto, and Y. Suzuki, Phys. Rev. Lett. **76**, 2242 (1996).
[30] Y. W. Yu, Z. Y. Zhang, P. N. Shen, and L. R. Dai, Phys. Rev. C **52**, 3393 (1995).
[31] H. X. Huang, P. Xu, J. L. Ping, and F. Wang, Phys. Rev. C **84**, 064001 (2011).
[32] L. Z. Chen, H. R. Pang, H. X. Huang, J. L. Ping, and F. Wang, Phys. Rev. C **76**, 014001 (2007).
[33] J. L. Ping, H. X. Huang, H. R. Pang, F. Wang, and C. W. Wong, Phys. Rev. C **79**, 024001 (2009).
[34] M. M. Xu, M. Yu, and L. S. Liu, Phys. Rev. Lett. **100**, 092301 (2008).
[35] M. Kamimura, Supp. Prog. Theo. Phys. **62**, 236 (1977).